

Supplementary information
Supplementary Table 1 Data collection and refinement statistics

	Vβ8.2 TCR-mCD1d- α-GalCer	Vβ7 TCR-mCD1d- α-GalCer	Vβ11 TCR-hCD1d-α- GalCer
Data collection			
Temperature	100K	100K	100K
Resolution limits (Å)	50-2.9 (3.06-2.90)	50-2.8 (2.95-2.80)	50-2.5 (2.59-2.50)
Space Group	P2 ₁ 2 ₁ 2 ₁	P2 ₁ 2 ₁ 2 ₁	P2
Cell dimensions (Å)	<i>a</i> =61.113, <i>b</i> =81.506, <i>c</i> = 233.451, $\alpha=\beta=\gamma=90.00^\circ$	<i>a</i> =58.229, <i>b</i> =81.913, <i>c</i> =243.253, $\alpha=\beta=\gamma=90.00^\circ$	<i>a</i> =112.11, <i>b</i> =82.36 <i>c</i> =117.18, $\alpha=90.00, \beta=101.3,$ $\gamma=90.00^\circ$
Total N ^o observations	149997	205387	195771
N ^o unique observations	26743	29526	66054
Multiplicity	5.6 (6.0)	7.0 (5.8)	3.0 (2.7)
Data completeness	100 (100)	99.7 (99.1)	91.1 (74.3)
I/ σ_1	11.1 (2.1)	13.7 (2.2)	10.5 (1.7)
R _{p.i.m} ¹ (%)	7.6 (31.5)	5.3 (30.4)	-
R _{merge} ² (%)	-	-	8.8 (34.3)
Refinement statistics			
R _{factor} ³ (%)	23.4	22.4	21.6
R _{free} ⁴ (%)	29.8	27.1	27.9
Non hydrogen atoms			
- protein	6559	6528	12995
- lipid	60	60	120
- water	28	47	494
- other	56	56	93
Ramachandran plot			
- Most favoured	88.9	91.6	89.4
- Allowed region (%)	11.1	8.3	10.1
- Generously allowed region (%)	0.0	0.1	0.5
B-factors (Å ²)			
- Average main chain	48.8	44.0	42.8
- Average side chain	49.0	44.3	42.5
- α-GalCer	52.1	49.0	29.7
- water	38.7	33.1	38.9
rmsd bonds (Å)	0.007	0.006	0.007
rmsd angles (°)	1.076	1.029	1.119

$$^1 R_{p.i.m} = \sum_{hkl} [1/(N-1)]^{1/2} \sum_i |I_{hkl,i} - \langle I_{hkl} \rangle| / \sum_{hkl} \langle I_{hkl} \rangle$$

$$^2 R_{merge} = \sum_{hkl} \sum_i |I_{hkl,i} - \langle I_{hkl} \rangle| / \sum_{hkl} \langle I_{hkl} \rangle$$

$$^3 R_{factor} = (\sum | |F_o| - |F_c| |) / (\sum |F_o|) - \text{for all data except as indicated in footnote 3.}$$

⁴ 5% of data was used for the R_{free} calculation

Values in parentheses refer to the highest resolution bin.

Supplementary Table 2 SPR data for NKT TCR interactions

Interaction	K_{on} ($M^{-1}s^{-1}$)	K_{off} (s^{-1})	$t_{1/2}$ (s)	K_D Calc. (nm)	χ^2	K_D obs. (nm)
V β 8.2 NKT- mCD1d- α -GalCer	6.40E+05	0.04	17.32	54.9	16.36	69.7
V β 8.2 NKT- hCD1d- α -GalCer	1.03E+06	0.09	7.7	84.9	7.21	93.9
V β 7 NKT- mCD1d- α -GalCer	4.26E+05	0.1	6.93	224	2.14	295
V β 7 NKT-hCD1d- α -GalCer	1.28E+05	0.49	1.41	3810	4.09	3420
hNKT TCR- mCD1d- α -GalCer	3.15E+05	0.33	2.1	1060	9.15	910
hNKT TCR-hCD1d- α -GalCer	6.27E+05	0.15	4.62	236	9.95	219

Supplementary Table 3 SPR data for mutant NKT TCR interactions

<u>Mutant</u>	<u>K_D (nM)</u>
Vβ7 wt	134
Vβ7 D26A	171
Vβ7 S54A	32.6
Vβ7 S56A	189
Vβ7 Y50F	520
Vβ7 E57A	225
Vβ8.2 wt	29.4
Vβ8.2 N28A	33.7
Vβ8.2 Y48F	> 1690
Vβ8.2 Y50F	377
Vβ8.2 E56A	165

Supplementary Figures

Suppl. Fig. 1. Characterisation of recombinant NKT TCRs

(A) Purified bacterially-expressed TCRs were analysed by SDS-PAGE under reducing conditions (lanes 1-4) and non-reducing conditions (lanes 5-8). Lanes 1&5 control TCR LC13, lanes 2&6 human V α 24V β 11 (NKT-15), lanes 3&7 mouse V α 14-V β 7 and lanes 4&8 mouse V α 14-V β 8.2.

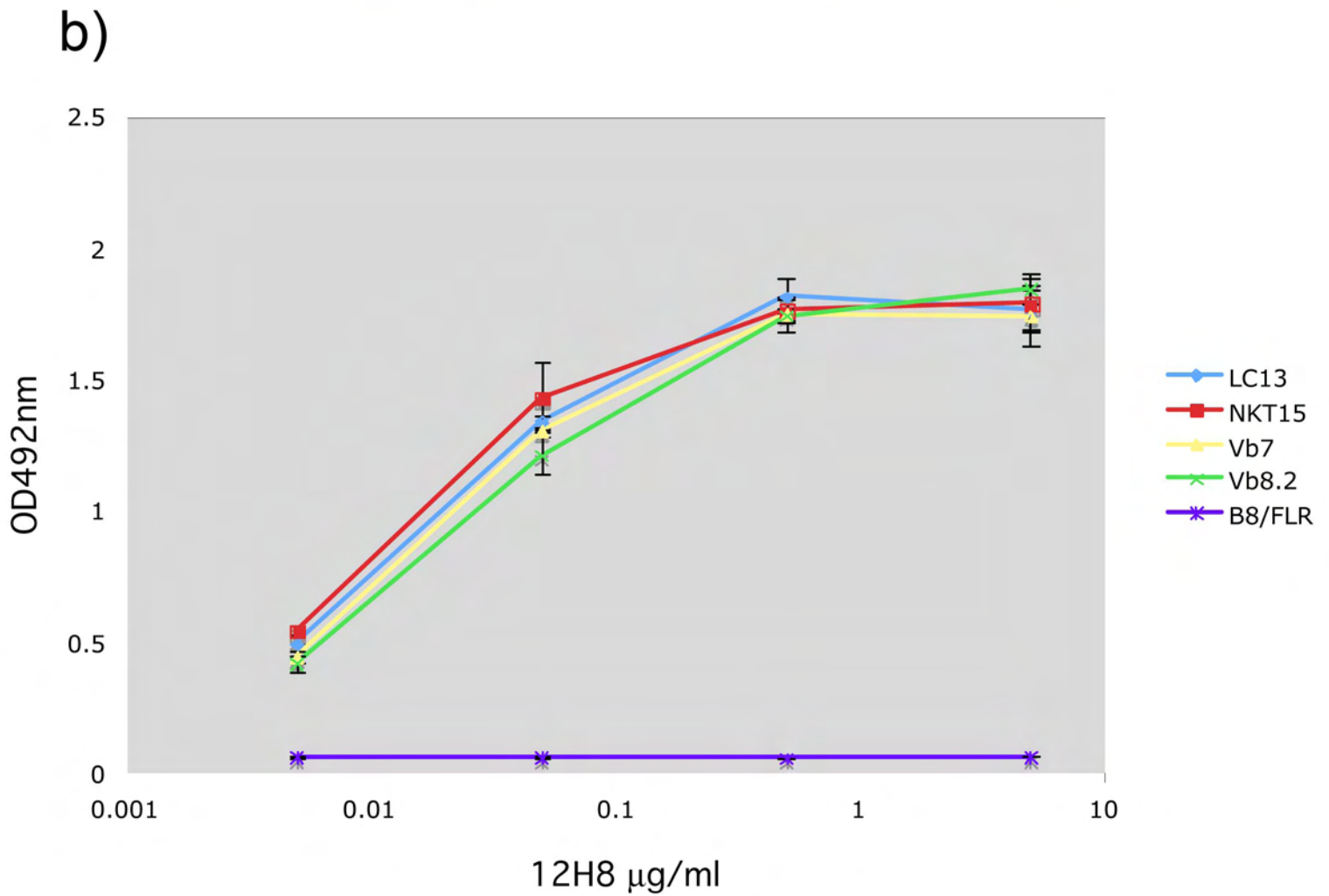
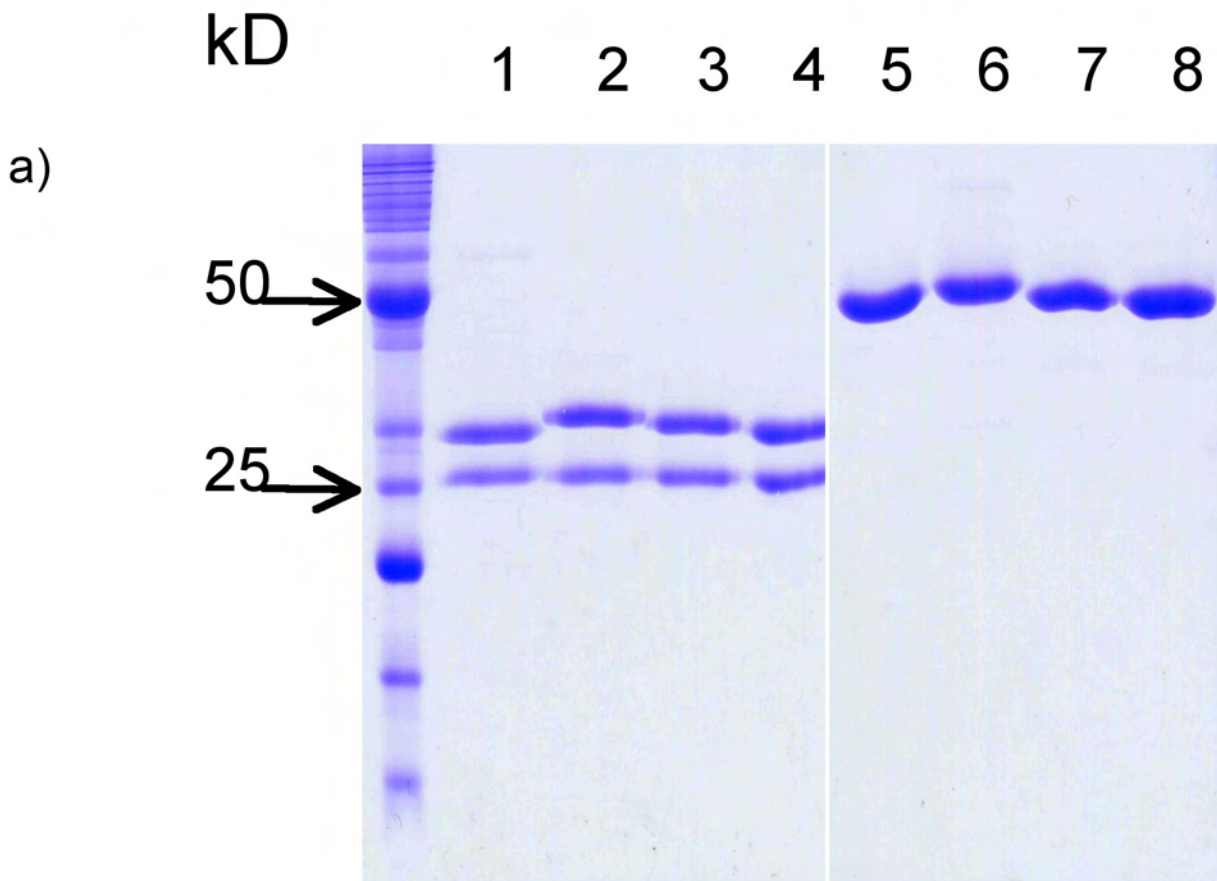
(B) The structural integrity of the constant domains of the recombinant soluble TCRs were assessed by using the conformationally-specific mAb, 12H8 in an ELISA. Plate bound TCRs, LC13 (positive control), human V α 24V β 11 NKT-15 TCR, mouse V α 14V β 7 TCR, mouse V α 14V β 8.2 TCR or irrelevant HLA B8-FLR (negative control) were treated with graded amounts of 12H8. 12H8-reactivity is shown as absorbance at 492nm on the vertical axis and concentration of 12H8 (μ g/ml) is indicated on the horizontal axis.

Suppl. Fig. 2 Shift in the position of the galactose head group of α -GalCer in mCD1d when ligated to the mouse NKT TCR. Mouse NKT TCR CDR1 α , purple; CDR3 α , yellow; mCD1d in ternary complex, grey; α -GalCer in ternary complex, magenta; mCD1d in binary complex, pink; α -GalCer in binary complex, green.

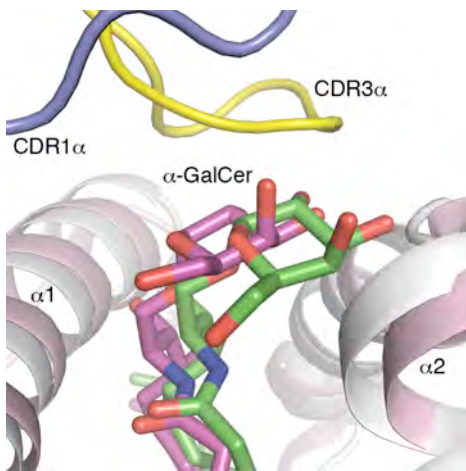
Suppl. Fig. 3 Sequence alignments between mouse and human NKT TCRs

Suppl. Fig. 4 Comparison of mouse NKT TCR-mCD1d- α -GalCer with human NKT TCR-hCD1d- α -GalCer. Parallel docking mode of the human and mouse NKT-TCR onto CD1d- α -GalCer. **(A)** Superposition of mouse V α 14-V β 8.2 NKT TCR-mCD1d- α -GalCer and human V α 24-V β 11 NKT TCR-hCD1d- α -GalCer. mTCR α -chain, cyan; mTCR β -chain, green; α -GalCer in mouse complex, magenta; mCD1d heterodimer, grey; hTCR α -chain, salmon; hTCR β -chain, yellow; α -GalCer in human complex, marine; hCD1d heterodimer, palegreen; **(B)** Superposition of mouse V α 14-V β 7 NKT TCR-mCD1d- α -GalCer and human V α 24-V β 11 NKT TCR-hCD1d- α -GalCer. mTCR β -chain, blue. mTCR α -chain, α -GalCer in mouse and human complex, mCD1d, hTCR and hCD1d colour coding as in **A**.

Supplementary Fig 1



Supplementary Figure 2



Supplementary Figure 3

		CDR1b						CDR2b																		
		26	27	28	29	30	31	48	49	50	51	52	53	54	55	56										
Mouse	Vb8.2	T	N	N	H	N	N	Y	S	Y	G	A	G	S	T	E										
Mouse	Vb7	D	M	S	H	E	T	I	S	Y	D	V	D	S	N	S										
Human	Vb11	T	M	G	H	D	K	Y	S	Y	G	V	N	S	T	E										
		CDR3b																								
		92	93	94	95	96	97	98	99	100	101	102	103							117						
Mouse	Vb8.2	C	A	S	G	D	A	G	G	N	Y	A	E	Q	F	F	G	P	G	T	R	L	T	V	L	
Mouse	Vb7	C	A	S	S	S	T	G	L	D	T	Q	Y	F	G	P	G	T	R	L	L	V	L	V	L	
Human	Vb11	C	A	S	S	G	L	R	D	R	G	L	Y	E	Q	Y	F	G	P	G	T	R	L	T	V	T
		CDR1a						CDR2a																		
		26	27	28	29	30	31	49	50	51	52	53	54													
Mouse	Va14	V	T	P	D	N	H	L	V	D	Q	K	D													
Human	Va24	V	S	P	F	S	N	M	T	F	S	E	N													
		CDR3a																								
		90	91	92	93	94	95	96	97	98	99	100	103	104	105	106	107	108	109	110	111	112	113	114	115	116
Mouse	Va14	C	V	V	G	D	R	G	S	A	L	G	R	L	H	F	G	A	G	T	Q	L	I	V	I	P
Human	Va24	C	V	V	S	D	R	G	S	T	L	G	R	L	Y	F	G	R	G	T	Q	L	T	V	W	P

Supplementary Figure 4

